Supporting Information

Yang et al. 10.1073/pnas.1706248114

SI Materials and Methods

Reagents used for the synthesis were purchased from Sigma-Aldrich and used without additional purification. Column chromatography was performed on silica gel (60 Å, 40–63 mm; SiliCycle Inc.) slurry packed into glass columns. Synthetic Aβ peptides (1–40/42) were purchased from rPeptide. Aggregates for in vitro studies were generated by the slow stirring of Aβ40 in PBS buffer (pH 7.4) for 3 d at room temperature. ^{1}H and ^{13}C NMR spectra were recorded at 300 and125 MHz, respectively, and reported in parts per million downfield from tetramethylsilane. Fluorescence measurements were carried out using an F-4500 fluorescence spectrophotometer (Hitachi). ROS is prepared following the previously reported protocol (24). Quantum yield was determined using an aqueous ICG solution as a standard (y = 0.01). Transgenic female APP-PS1 mice and age-matched WT female mice were purchased from Jackson Laboratory. All animal experiments were approved by the Institutional Animal Use and Care Committee at Massachusetts General Hospital.

Synthesis of CRANAD-61. CRANAD-5 was synthesized according to our procedure and other previously reported procedures (43). To a solution of CRANAD-5 (100 mg, 0.276 mmol) in acetone (3.0 mL), $B(OH)_3$ (20 mg, 0.32 mmol) was added followed by the addition of oxalic acid (70 mg, 0.55 mmol, 2 eq). The resulting solution was stirred at room temperature for 18 h. After removing the solvent, the residue was purified with a flash column (hexane/ethyl acetate/dichloromethane = 2:1:1) to give a blue powder CRANAD-61 (45) (40 mg, yield: 31.4%). ^{1}H NMR (DMSO-d_6) δ (parts per million) 3.14 (s, 12H), 6.45 (s, 1H), 6.85–6.93 (m, 6H), 7.75 (d, J = 8.5 Hz, 4H), 7.96 (d, J = 15 Hz, 2H). ^{13}C NMR (DMSO-d_6) δ (parts per million) 40.53, 101.28, 112.64, 113.93, 122.36, 132.98, 148.18, 153.78, 158.91, and 175.0. Electrospray ionization mass spectrometer (M + H) m/z = 461.2.

Stability Testing for CRANAD-61. The stability of CRANAD-61 was tested in different solutions, including PBS buffer solutions at pH 6.0, 6.7, 7.0, and 7.4 and 20% DMSO PBS (pH 7.4). Solutions of CRANAD-61 (250 nM) at the above pH and cosolvent were added to a 96-well plate (n = 5 for each pH and DMSO cosolvent), and then, the plate was subjected to imaging using an IVIS Spectrum imaging system (Perkin-Elmer) after 0, 2, 5, 10, 20, 30, and 60 min of incubation at 37 °C (Ex = 675 nm and Em = 740 nm). For quantification, the signals at different time points were normalized to the signal at 0 min of incubation.

Fluorescence Spectral Testing of CRANAD-61 with ROS. To record the fluorescence response of CRANAD-61 with different ROS, the following procedure was utilized. In step 1, 1.0 mL of PBS buffer with 20% DMSO was added to a quartz cuvette as a blank control, and its fluorescence was recorded with the same parameters as for CRANAD-61. In step 2, the fluorescence Em spectrum of a CRANAD-61 solution (1.0 mL, 250 nM) was recorded with Ex at 460 and 650 nm and Em from 480 to 900 nm and from 680 to 900 nm, respectively. In step 3, to the above incubated CRANAD-61 solution, 10 μL ROS (H_2O_2 as representative species) of different concentrations was added. The Em spectra at different time points were recorded (Ex = 460 nm, Em = 480–900 nm and Ex = 650 nm, Em = 680–900 nm). The final spectra from steps 2 and 3 were corrected using the blank control from step 1.

Time Course Recording of CRANAD-61 with ROS. To a 1.0 mL solution (20% DMSO PBS, pH 7.4) of CRANAD-61 (2.5 μM), 10 μL ROS was added (H_2O_2 as representative species; final concentration was 2.5 μM). The Em spectra were recorded (Ex = 460 nm, Em = 480–900 nm) at 0, 1, 5, 10, and 15 min after ROS addition. In addition, we also recorded the spectra of a 2.5 μM solution of CRANAD-61 without ROS at the above time points. The fluorescence intensity (F.I.) changes were calculated based on the intensities at 570 nm from the two spectra of the solutions with and without ROS at the same time points.

Concentration Dependency of CRANAD-61 with ROS. To solutions (20% DMSO PBS, pH 7.4) of CRANAD-61 (250 nM), 10 μL ROS was added to make the final concentrations of 0, 5, 100, 250, 500, 1,000, 2,500, and 5,000 nM. The Em spectra were recorded (Ex = 460 nm, Em = 480–900 nm) at 15 min after the ROS addition. The F.I. changes with different ROS concentrations were calculated via subtracting the intensity at 570 nm of solutions without ROS after 15 min of incubation.

Aβ40/42 Monomer and Aggregates Preparation. These Aβ species were prepared according to our previously reported procedure (44, 50).

Fluorescence Spectra of CRANAD-61 with Aβ Species. To solutions (5% DMSO PBS, pH 7.4) of CRANAD-61 (250 nM), 10 μL of an Aβ40 aggregates solution was added to the final concentration of 250 nM. The Em spectra were recorded (Ex = 650 nm, Em = 680–900 nm) after 2 min of incubation. Note that 20% DMSO PBS solution was not suitable for testing with Aβ species, because the high DMSO content could lead to disassociation of Aβ aggregates and oligomers.

K_d Measurements for CRANAD-5 and CRANAD-61 with Aβ Species. The measurements were conducted according to our previously reported procedure (44, 50). For CRANAD-5, Ex = 465 nM and Em = 560 nM were used. For CRANAD-61, Ex = 670 nM and Em = 740 nM were used.

Effects of Metal Ions and H_2O_2 on Fluorescence of CRANAD-61 with Aβ Aggregates. To solutions of CRANAD-61 (250 nM in 5% DMSO PBS, pH 7.4) in a 96-well plate, a solution of $CuSO_4$ was added to each well to a final Cu^{2+} concentration of 250 nM (n = 6). Similarly, solutions of $FeCl_2$ and $FeCl_3$ were added to the wells (n = 6). After 15 min of incubation at 37 °C, the plate was imaged using an IVIS imaging system (Ex = 675 nm and Em = 740 nm). For quantification, the signals from the wells containing metal ions were normalized to the signal of CRANAD-61 without metal ions. To test the effect of metal ions on the fluorescence of CRANAD-61 with Aβ40 aggregates, a similar procedure was used, except that a solution of Aβ40 aggregates (250 nM) was added to each well with CRANAD-61 solution. For quantification, the signals from the wells containing metal ions were normalized to the signal of CRANAD-61 + Aβ without metal ions. To test the effects of H_2O_2 on the fluorescence of CRANAD-61 in the presence of Aβ species, a solution of H_2O_2 (250 nM) was added to the wells containing CRANAD-61, metal ions, and Aβ40 aggregates. The plate was then imaged at 0, 15, and 30 min after incubation. For quantification, the signals from the wells containing metal ions + H_2O_2 at different time points were normalized to the signal from the same well after 0 min of incubation.

Particle Size Measurement and Transmission Electron Microscope Imaging of CRANAD-61. Solutions of CRANAD-61 (2.5 μM) were prepared in 5 and 20% DMSO PBS (pH 7.4). Particle size

measurements were performed on a particle size analyzer (Zetasizer Nano; Malvern Instruments). For transmission electron microscope (TEM) imaging, 5 μL of the prepared sample was dropped to a Formvar-coated TEM grid followed by the addition of 2 μL of a phosphotungstic acid (PTA) contrast solution. After 1 min, the liquid on the grid was carefully dried with a corner of the filter paper, and the resulting grid was further dried in the air for 2–5 min. TEM images were obtained with a JEM 1011 electron microscope (JEOL).

Log *P* Measurement. CRANAD-61 (250 μM) in octanol (1.5 mL) was subjected to partition with octanol-saturated water (1.5 mL). The resulting mixture was stirred vigorously for 5 min and centrifuged at 3000 × *g* for 5 min. The octanol layer was separated, and its fluorescence spectrum was recorded (Ex = 650 nm). The above water layer was partitioned with water-saturated octanol (1.5 mL); the octanol layer was separated after 5 min of vigorous stirring and 5 min of centrifugation at 3000 × *g*, and its spectrum was recorded. The log *P* value was calculated using the F.I. ratio at 810 nm for the above two octanol extractions.

Quantum Yield. The solutions of CRANAD-61 and ICG (2.5 μM in PBS as the standard solution) were prepared, the absorbance of each was determined using the Spectra max M2 Micro Plate Reader, and the Em spectra of these solutions were recorded using the F-4500 Fluorescence Spectrophotometer. Quantum yield was calculated using the equation $\Phi_{F(X)} = (A_s/A_x)(F_x/F_s)(n_x/n_s)^2\Phi_{F(S)}$, where Φ_F is the fluorescence quantum yield, A is the absorbance at the Ex wavelength, F is the area under the corrected Em curve, and n is the refraction index of the solvents used. Subscripts s and x refer to the standard and the unknown, respectively. The absorbance values at 675 nm from CRANAD-61 and ICG and the areas under Em curves from 700 to 900 nm (Ex = 675 nm) were used for quantum yield calculation. Two duplicated samples were used for the measurement.

The Parallel Artificial Membrane Permeability Assay–BBB. The stock solution of CRANAD-61 (5 mg/mL) in DMSO was prepared. Ten microliters of stock solution was diluted to 25 μg/mL with 5% DMSO to prepare a test solution. Test solution was added to every donor well (300 μL per well), and next, the acceptor well was soaked with 4 μL Porcine Polar Brain Lipid (20 mg/mL) in dodecane; then, 200 μL of PBS was added. The acceptor well was placed onto the donor well to form the "sandwich" structure and incubated at the room temperature for 18 h. After removal of the acceptor well, the donor and acceptor solutions (150 μL each) were measured using the Spectra max M2 Micro Plate Reader, and permeability (P_e) was calculated using the formula (51)

$$P_e = -\frac{V_{dn}V_{ac}}{st(V_{dn}+V_{ac})}\ln\left\{1-\frac{[drug]_{ac}}{[drug]_{ref}}\right\},$$

where V_{dn} (milliliters) = volume of donor well, V_{ac} (milliliters) = volume of acceptor well, $[drug]_{ac}$ = OD value of the acceptor well, $[drug]_{ref}$ = OD value of the reference drug (Verapamil), s (centimeters^2) = area of the membrane, and t (seconds) = incubation time.

Phantom Imaging with NIRF Parameters. To 200 μL solutions (5% DMSO PBS, pH 7.4) of CRANAD-61 (250 nM) on a 96-well plate, 10 μL H_2O_2 was added to make the final concentrations of 0, 5, 100, 250, 500, 1,000, and 2,500 nM (n = 3 for each concentration). NIRF imaging was conducted at 15 min after H_2O_2 addition with Ex = 675 nm, Em = 740 nm, and field of view (FoV) = C. For mouse brain homogenate NIRF imaging, 10 μL H_2O_2 was added to a 0.5-mL brain homogenate (20.0 mg) containing CRANAD-61 (250 nM) to make the final concentration of 250 nM (n = 3). After 15 min of incubation, NIRF imaging was conducted with the same imaging parameters as above. Solutions of homogenate containing CRANAD-61 without H_2O_2 were used as controls.

BBB Penetration. BALB/c mice were i.v. injected with CRANAD-61 (8.0 mg/kg). After 30 min, mice were perfused with saline solution, and the brains were excised. The brain samples were homogenized in 2.0 mL water followed by the addition of ethyl acetate (2.0 mL). The resulting homogenate was stirred for 2 h and centrifuged for 5 min at 3750 × *g*. The extractions were subjected to fluorescence spectral recording.

Histological Staining with CRANAD-61. A 25-μm brain slice from an 18-mo-old APP/PS1 mouse was fixed with 4% formalin for 5 min and washed with distilled water twice for 5 min. The slice was incubated with CRANAD-61 solution (25.0 μM in 25% ethanol and 75% dd water) for 15 min and then, washed with 20% ethanol followed by washing with dd water. After drying, the same slide was incubated with Thioflavin S (52, 54) (25.0 μM in 25% ethanol and 75% dd water) for 5 min and then, washed three times with dd water. After drying, the slice was covered with VectaShield mounting media. Florescence images were obtained using the Nikon Eclipse 50i microscope in red and green channels.

Two-Photon Imaging of AD Mouse. Two days before imaging, an APP-PS1 mouse (14 mo old) was injected with 7.5 mg/kg of amyloid dye FSB (CAS 760988–03-2, dissolved in 10% DMSO with PBS; Santa Cruz). Note that FSB could remain stably bound to amyloid plaques for at least 90 d after injection (10). On the imaging day, the mouse was anesthetized with ketamine/xylazine (70 mg/12.5 mg/kg), and a 4.0-mm cranial imaging window was surgically prepared on one hemisphere around somatosensory cortex. Before CRANAD-61 injection, two-photon (Prairie Technologies) images were collected using 800-nm Ex and 420- to 460-nm Em for FSB fluorescence. Spherical structures with fibrous edges and surrounding lipofuscin autofluorescence were identified as amyloid plaques, and discontinuous ring-like structures along the blood vessels were identified as CAAs. Three 420 × 420-μm FoVs were selected with abundant amyloid deposits within the cranial window. CRANAD-61 (2.0 mg/kg in a fresh solution containing 15% cremorphor, 15% DMSO, and 70% PBS) was then injected i.v. by a bolus injection. The above three FoVs were relocated and imaged with 900-nm Ex and green (500–550 nm) and red (640–680 nm) Ems. The same regions were then imaged with the same laser and detector settings at 5, 20, and 60 min after dye injection at 1,024 × 1,024-pixel resolution. All images were collected using a 20× water immersion objective (N.A. 1.0; Zeiss).

To quantify the fluorescence change of individual amyloid deposits, the outlines of plaques and CAAs were traced manually in the FSB *Z*-stack images. CAAs on the vessel segment between the two branch points were considered as a single deposit. Ten plaques and CAAs were measured at each time point using the traced regions of interest (ROIs) for red and green fluorescence channels. Wilcoxon matched pairs signed rank test was used for statistical comparison between 5- and 60-min time points.

Whole-Brain NIRF Imaging of ROS in AD. In vivo NIRF imaging was performed using an IVIS Spectrum imaging system. Image processing and analysis were performed using Living Image 4.2.1 software (Perkin-Elmer). Images were acquired with a 640-nm Ex filter and a 720-nm Em filter. The heads of female APP-PS1 transgenic mice of different ages (4, 12, and 18 mo, n = 3–5) and age-matched WT control female mice (n = 3–5) were shaved before background imaging. An injection solution of CRANAD-61 (4.0 mg/kg) was

freshly prepared in 15% DMSO, 15% cremorphor, and 70% PBS and stabilized for 20 min before i.v. injection. Each mouse was i.v. injected with 100 μL of CRANAD-61. NIRF signals from the brain areas were recorded at 0, 30, 60, 120, and 240 min after the injection. To quantify the NIRF signal, an equal-sized ROI was drawn around each brain region.

Measurement of ROS Levels in the Blood of AD and Control WT Mice. To 200 μL solutions (5% DMSO PBS, pH 7.4) of CRANAD-61 (250 nM) on a 96-well plate, 5 μL freshly drawn blood from APP/PS1 and WT mice was added to each well ($n = 3$). NIRF imaging was conducted at 1 and 5 min after incubation with the following parameters: Ex = 675 nm, Em = 740 nm, and FoV = C.

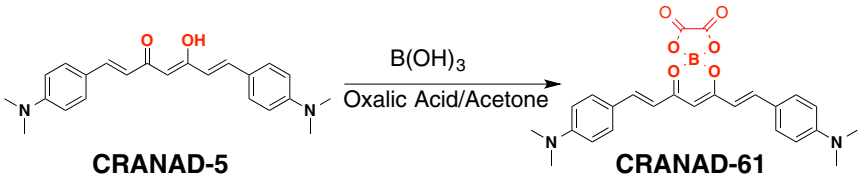

Fig. S1. Synthetic scheme of CRANAD-61.

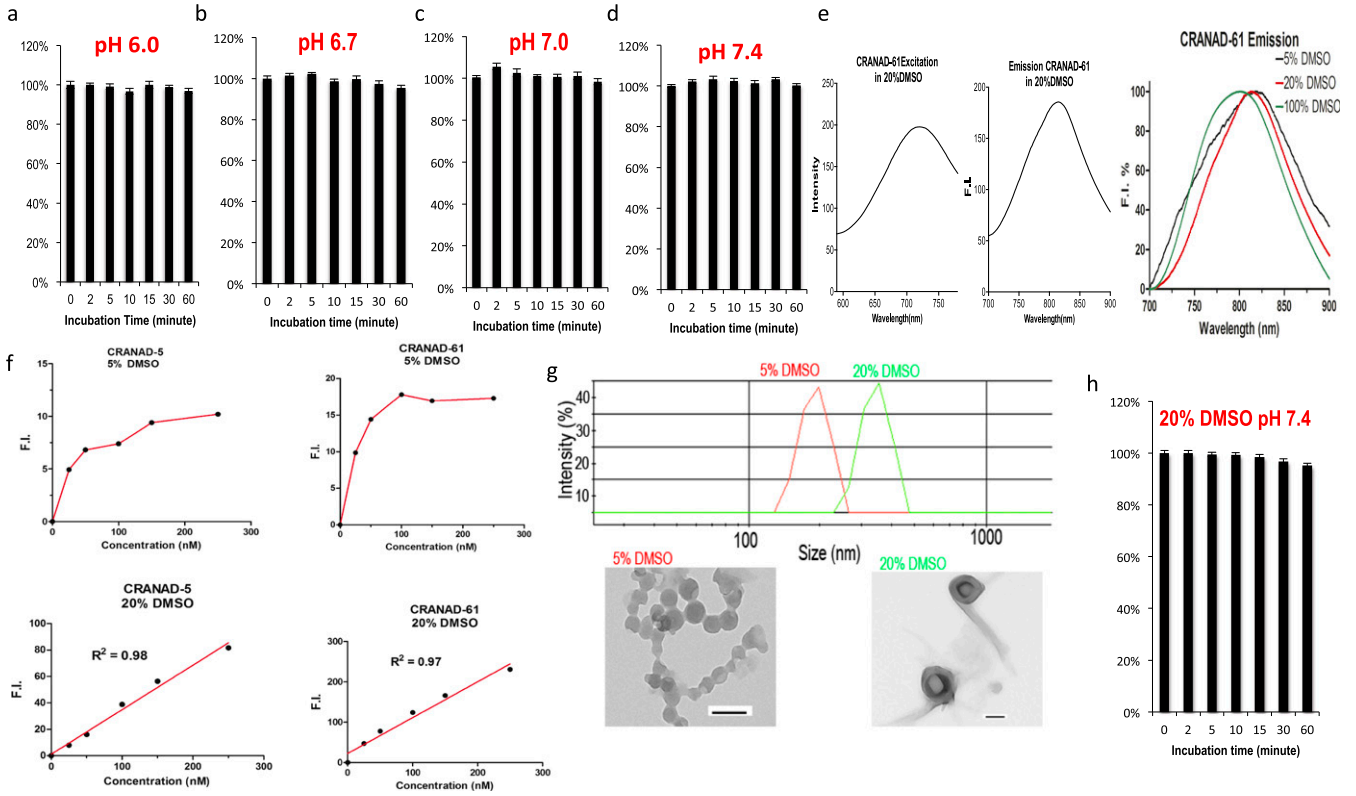

Fig. S2. (*A–D*) Stability testing of CRANAD-61 in PBS at different pH values. No apparent F.I. decreases could be observed during 60-min incubation at 37 °C. (*E*) Ex and Em spectra of CRANAD-61 in 20% DMSO PBS solution and Em spectra of CRANAD-61 in 5, 20, and 100% DMSO solutions. (*F*) F.I. titrations with CRANAD-5 and CRANAD-61 in 5 and 20% DMSO solutions. Significant quenching effects and narrow linear ranges could be observed in 5% DMSO solutions, and no apparent quenching and excellent linear fittings could be seen in 20% DMSO solutions. (*G*) Particle size measurements and TEM images of CRANAD-61 PBS solutions in 5% DMSO (red) and 20% DMSO (green). (Scale bar: 100 nm.) (*H*) Stability testing of CRANAD-61 in 20% DMSO PBS (pH 7.4) during 60 min of incubation at 37 °C. A slight decline (5%) in intensity could be observed after 60 min of incubation.

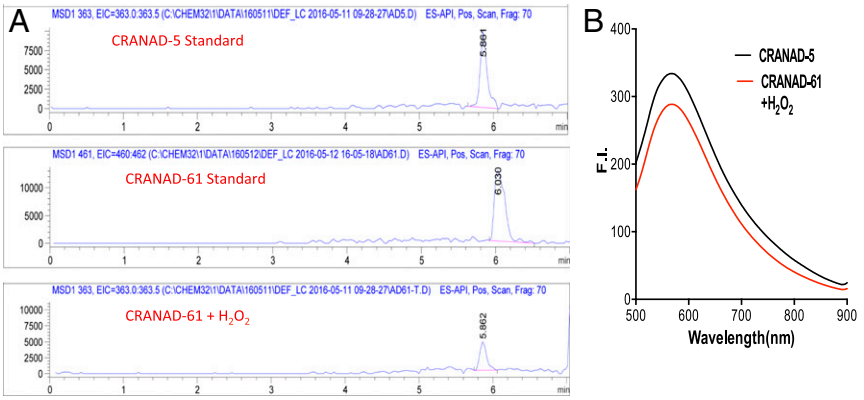

Fig. S3. (*A*) LC-MS of CRANAD-5, CRANAD-61, and the reaction mixture containing CRANAD-61 + H_2O_2. (*B*) Fluorescence spectra of CRANAD-5 and the reaction mixture at Ex = 460 nm.

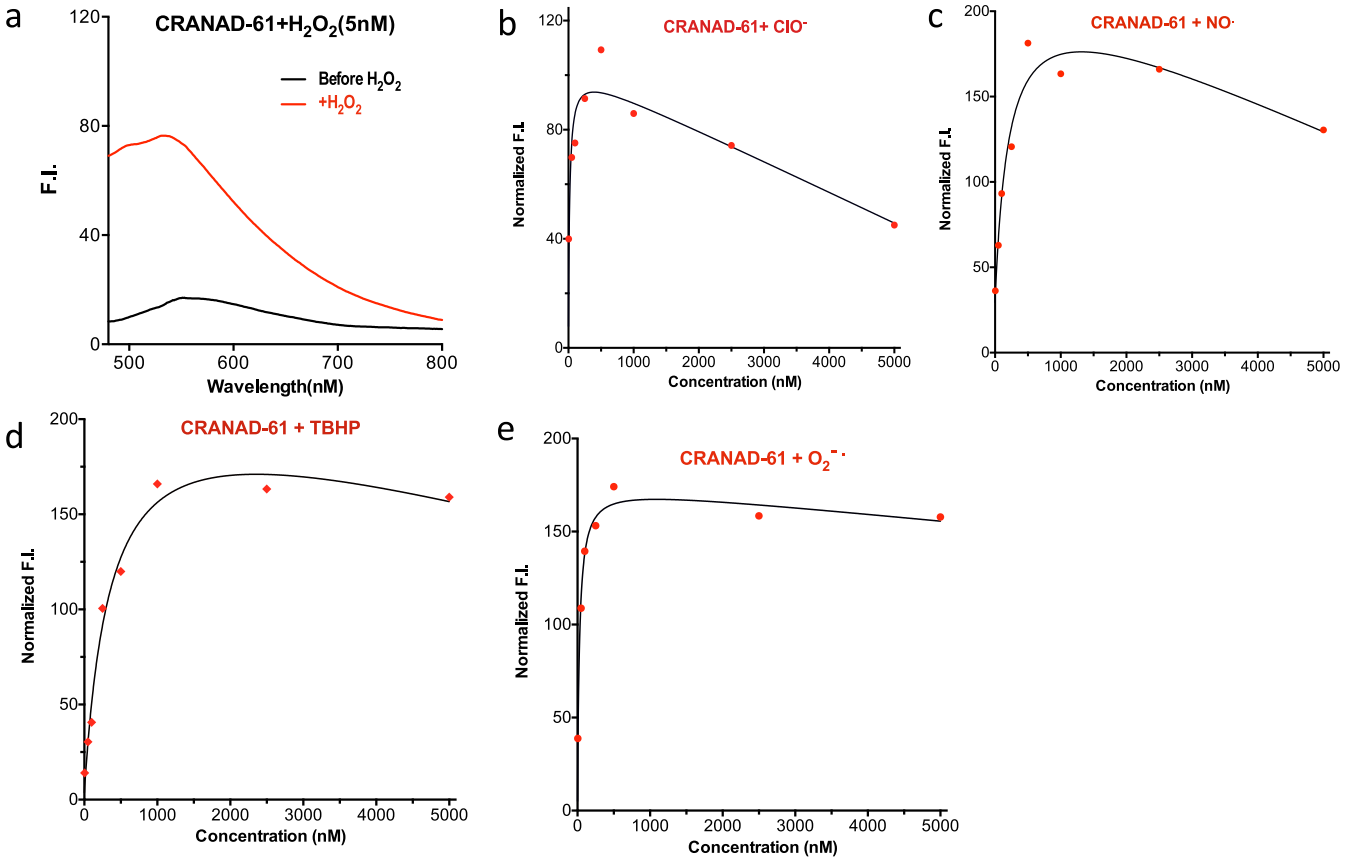

Fig. S4. (*A*) Fluorescence changes of CRANAD-61 with 5.0 nM H_2O_2 (Ex = 460 nm). (*B–E*) Concentration-dependent intensity changes of CRANAD-61 (250 nM) with different ROS. High concentrations of ROS could lead to photobleaching as evidenced by the decrease of F.I. at high concentrations of ROS.

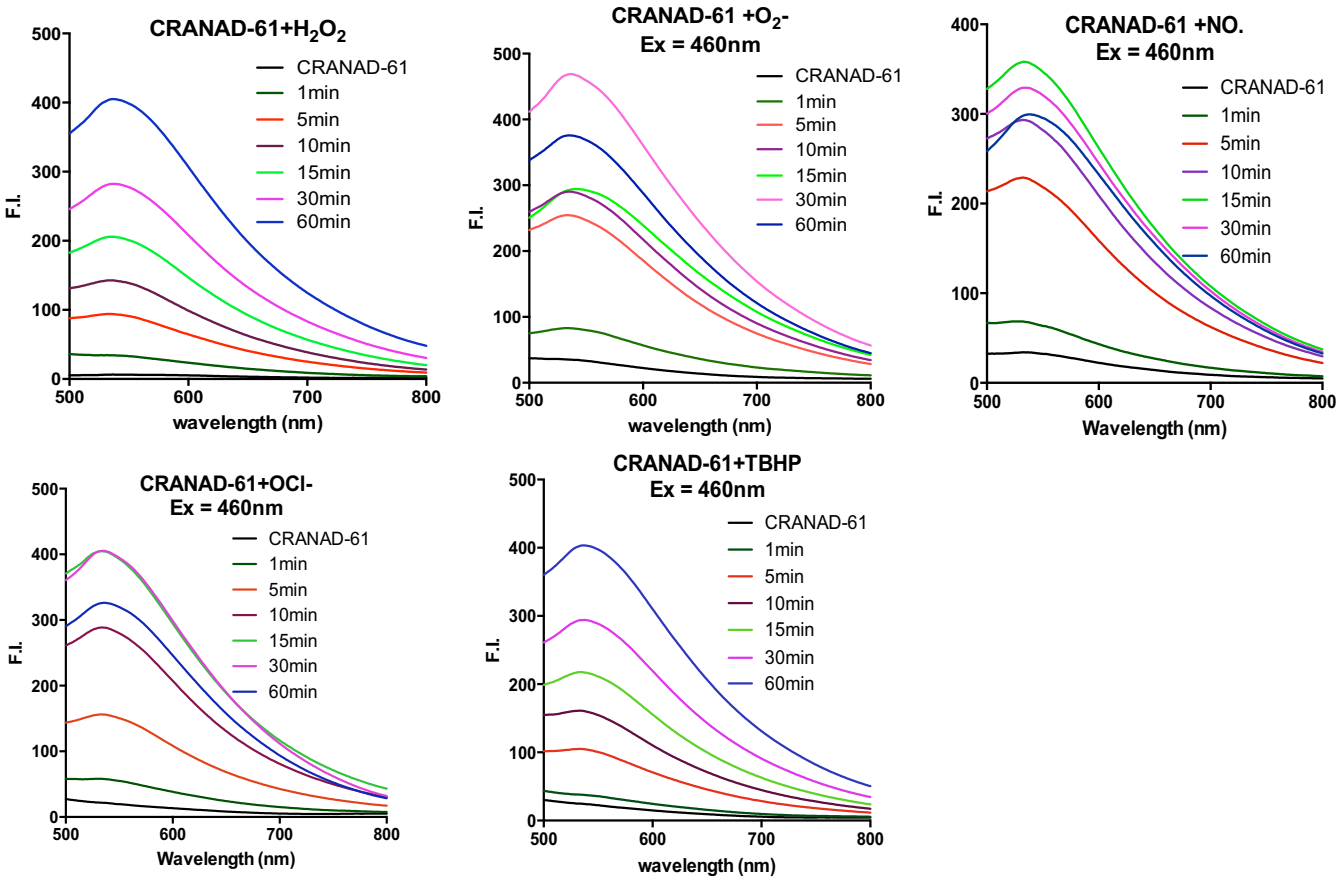

Fig. S5. Fluorescence response of CRANAD-61 (2.5 μM) with various ROS (2.5 μM) at different incubation times (Ex = 460 nm).

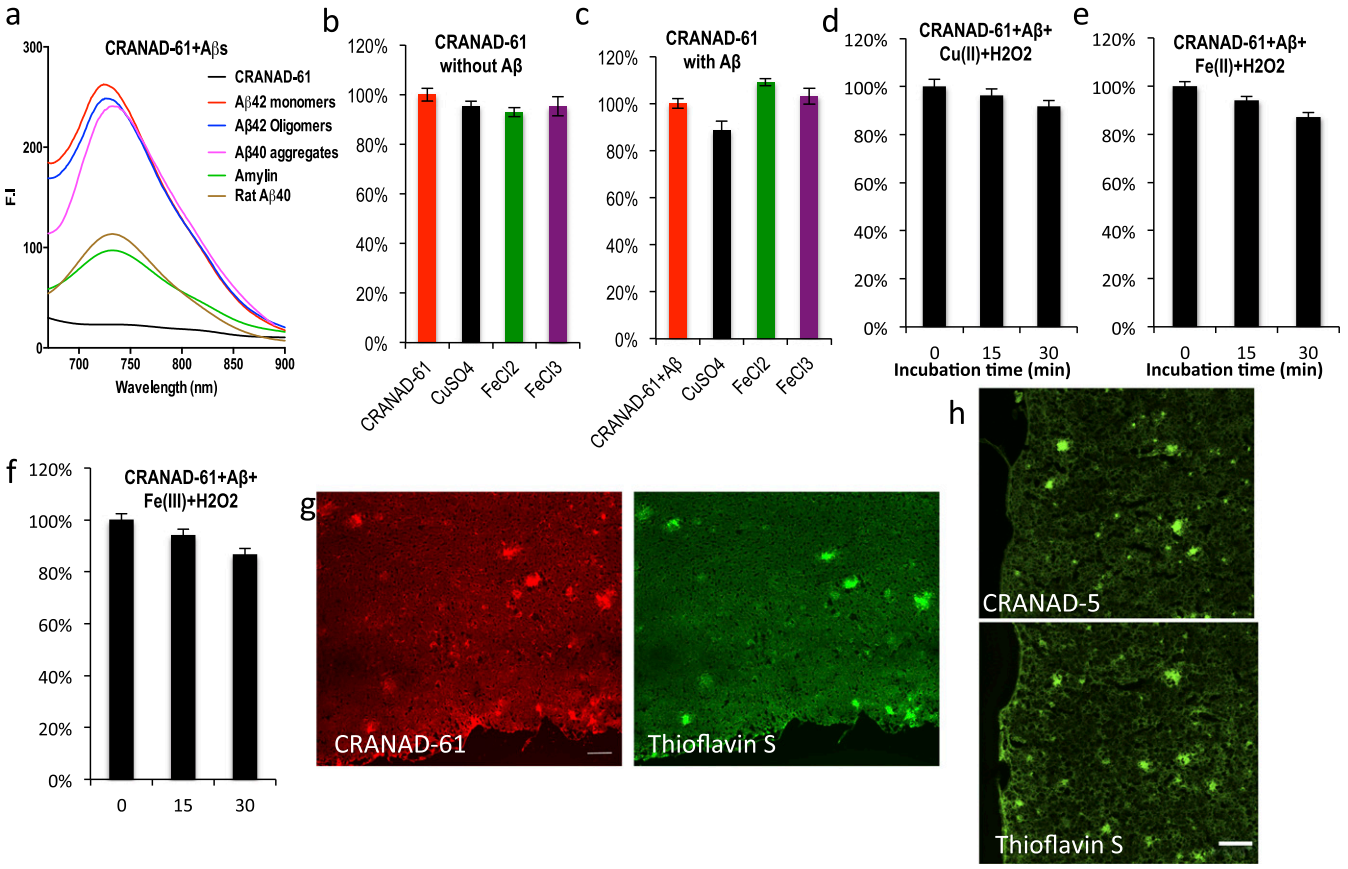

Fig. S6. (*A*) Fluorescence spectra of CRANAD-61 with different Aβ species (Ex = 675 nm), including Aβ40 aggregates, Aβ42 monomers, Aβ42 oligomers, rat Aβ40, and amylin. The data indicated that CRANAD-61 had certain specificity toward Aβs over rat Aβs and amylin, an aggregation-prone 37-residue peptide. (*B* and *C*) Quenching effects of metal ions on the fluorescence of CRANAD-61 alone and CRANAD-61 + Aβs. (*D–F*) Quenching effects of metal ions on the fluorescence of CRANAD-61 + Aβs in the presence of H_2O_2. (*G*) Histological staining of a brain slice from a 14-mo-old APP/PS1 mouse with Thioflavin S (*Right*) and CRANAD-61 (*Left*). (Scale bar: 50 μm.) (*H*) Histological staining of two consecutive brain slices from a 14-mo-old APP/PS1 mouse with CRANAD-5 (*Upper*) and Thioflavin S (*Lower*). (Because the Ems of both CRANAD-5 and Thioflavin S are in the green filter range, costaining was not feasible, and thus, two consecutive slices were used.) (Scale bar: 50 μm.)

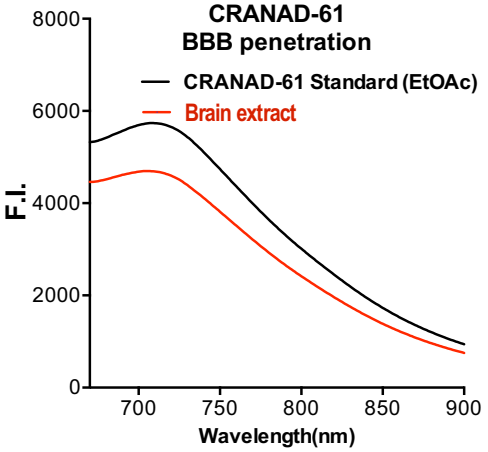

Fig. S7. Fluorescence spectra of standard CRANAD-61 (black) and brain extract (red; Ex = 675 nm).

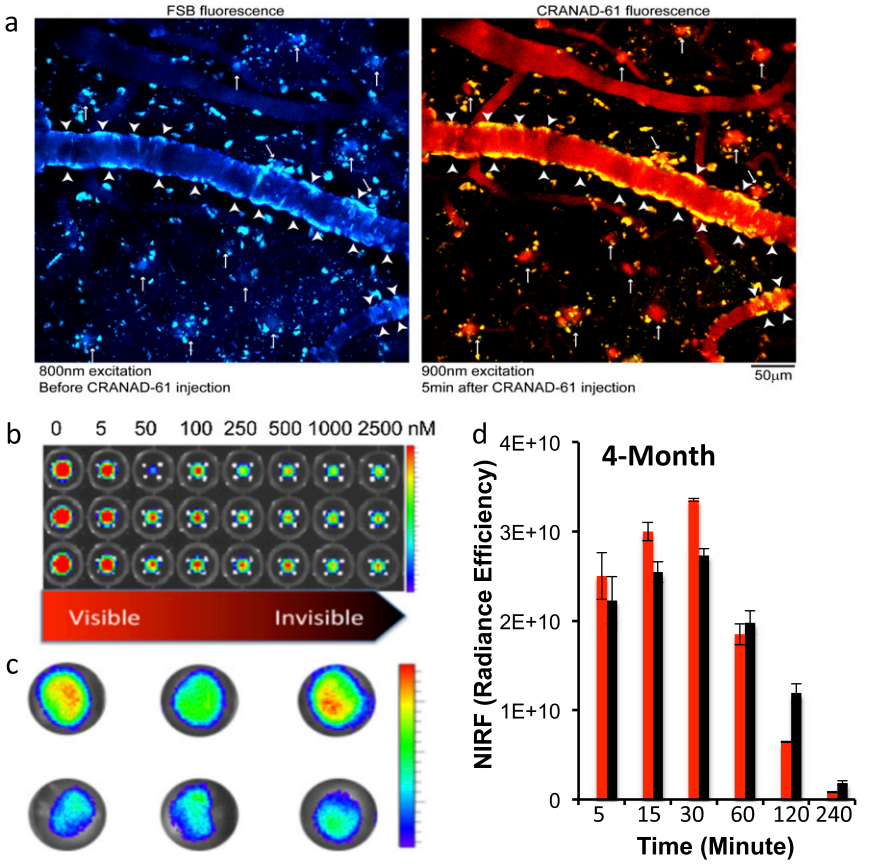

Fig. S8. (*A*) Two-photon images of CRANAD-61 labeling in an APP-PS1 mouse showed specific amyloid affinity. The same FoV as imaged before (*Left*; 420- to 460-nm Em for FSB fluorescence, a widely used specific dye for Aβ plaques and CAAs) and after CRANAD-61 injection (*Right*). Yellow color was from the merged signals in green and red channels. Green indicates 500- to 550-nm Em and red indicates 640- to 680-nm Em for CRANAD-5 and CRANAD-61 fluorescence, respectively. Arrows indicate the locations of amyloid plaques, and arrowheads indicate the CAAs. Note the absence of CAAs in the vessels in the upper part of the image and partial coverage of CAAs in the vessel in the lower right corner. (*B*) In vitro imaging of CRANAD-61 with H_2O_2 at different concentrations (Ex = 675 nm, Em = 740 nm; performed in triplicate). Note the "visible to invisible" transformation in the NIR imaging window. (*C*) Phantom imaging of mouse brain homogenates with CRANAD-61 (*Upper*) and H_2O_2 (*Lower*; performed in triplicate). (*D*) NIRF signal from 4-mo-old APP/PS1 and age-matched control mice after i.v. injection of CRANAD-61.

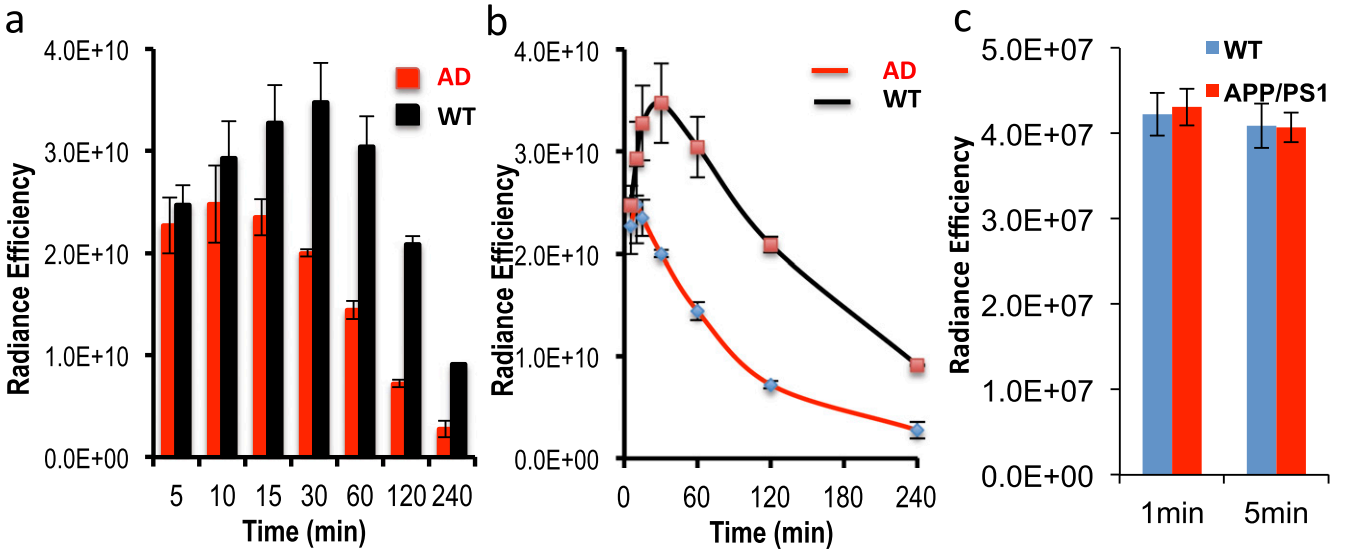

Fig. S9. (*A*) Bar graph of NIRF signals at different time points from 18-mo-old APP/PS1 and age-matched control mice after i.v. injection of CRANAD-61 ($n = 3$). (*B*) Time course plot of the same data from *A*. An apparent time point difference for the maximal NIRF signals in AD and WT mice (10 vs. 30 min) could be observed, and two-phase signal decay could be seen in the AD group. (*C*) NIRF signal in blood from APP/PS1 mice and control WT mice after i.v. injection of CRANAD-61. There was no significant difference in the signals from the blood between APP/PS1 and WT mice.

Table S1. Representative ROS probes from references, their properties, and applications

Name	Ex/Em	ROS	In vitro	In vivo imaging	CNS imaging	Concentration range	Response time (min)	Ref.
CF-SPN	580/680, 680/820	H_2O_2, $ONOO^-$	Yes	Yes	No	~1 μM	~1	19
MitoPY1	498/540	H_2O_2	Yes	No	No	100 μM to 10 mM	Not applicable	21
NBzF	495/520	H_2O_2	Yes	No	No	5 μM	~15	23
MitoAR	553/574	ROS	Yes	No	No	5–100 μM	<1	24
QCy7	560/715	H_2O_2	Yes	Yes	No	~1 μM	Not applicable	25
pnGFP	460/520	$ONOO^-$	Yes	No	No	~10 μM	~60	26
HO-mito-Etd	396/510	O_2^-	Yes	No	No	~1 μM	~1	27
MMSiR	620/660	ROS	Yes	Yes	No	5–1,000 μM	<1	28
PIS	378/505	OCl^-	Yes	No	No	1 μM	2 h (cell)	29
CyPSeO	758/790	$ONOO^-$	Yes	No	No	~10 μM	~10	30
Lyso-NINO	440/530	NO	Yes	No	No	10 μM	~60	31
PN600	555/600	$ONOO^-$	Yes	No	No	~10 μM	Not applicable	32
BOTI	450/510	HNO	Yes	No	No	~1 mM	~60	33
Hydro-IR-676	675/693	ROS	Yes	Yes	No	~100 nM	~1	34